Theor Chem Acc (2012) 131:1151
DOI 10.1007/s00214-012-1151-9

REGULAR ARTICLE

A relativistic DFT study of magnetic exchange coupling in ketimide bimetallic uranium(IV) complexes

Samir Meskaldji · Abdellah Zaiter · Lotfi Belkhiri · Abdou Boucekkine

Received: 23 July 2011 / Accepted: 13 September 2011 / Published online: 15 February 2012

Abstract Magnetic exchange couplings in bis(ketimide) binuclear U^{IV}/U^{IV} complexes $[Cp'_2UCl]_2$(μ-ketimide) diuranium(IV) and $[(C_5H_5)_2(Cl)An]_2$(μ-ketimide) ($Cp' = C_5Me_4Et$; ketimide = N=CMe-(C_6H_4)-MeC=N) have been investigated computationally using relativistic density functional theory (DFT) combined with the broken symmetry (BS) approach. Using the B3LYP hybrid functional, the BS ground state of these U^{IV}/U^{IV} $5f^2$–$5f^2$ complexes has been found of lower energy than the high spin (HS) quintet state, indicating an antiferromagnetic character (estimated coupling constant $|J| < 5$ cm^{-1}) which has not yet been evidenced unambiguously experimentally. On the contrary, the BP86 GGA functional overestimates greatly the antiferromagnetic character of the complexes ($|J| > 100$ cm^{-1}). As recently reported for para-bis(imido) $[(C_5H_5)_3U]_2$ (μ-imido) uranium(V) complex, spin polarization is mainly responsible for the antiferromagnetic coupling through the π-network orbital pathway within the bis(ketimide) bridge. Furthermore, spin polarization is exalted by the combined roles of the 5*f* metal orbitals and of the π-conjugated ketimide bridging ligand which permit electronic communication between the two uranium atoms albeit separated by a distance of the order of 10 Å. The MO analysis clarifies which MOs contribute to the antiferromagnetic coupling in the binuclear complexes under consideration and brings to light the 5*f* orbitals driving contribution.

Keywords Ketimide biuranium(IV) complexes · Magnetic exchange coupling · ZORA/B3LYP · Broken symmetry

Dedicated to Professor Vincenzo Barone and published as part of the special collection of articles celebrating his 60th birthday.

S. Meskaldji · A. Zaiter · L. Belkhiri (✉)
URCHEMS, Université Mentouri de Constantine,
25017 Constantine, Algeria
e-mail: lotfi.belkhiri@umc.edu.dz

S. Meskaldji
ENSET, 21000 Skikda, Algeria

A. Boucekkine (✉)
Laboratoire Sciences chimiques de Rennes,
UMR CNRS 6226, Université de Rennes 1,
Campus de Beaulieu, 35042 Rennes Cedex, France
e-mail: abdou.boucekkine@univ-rennes1.fr

1 Introduction

Since the first report of the single-molecular magnetic compound with the Cu_2Gd core in 1985 [1], the chemistry of this new class of fascinating transition d-metals and lanthanide containing materials continue to attract much attention at both experimental [1–14] and theoretical [15–46] levels. Molecules containing a finite number of interacting spin centres (e.g. paramagnetic ions) connected through a bridging ligand provide ideal opportunities to study basic concepts of magnetism, for example, superexchange interactions as early expressed by Kahn [47]. They constitute model compounds for the development of single-molecule magnets (SMM) and multifunctional materials [4–6].

From a theoretical point of view, quantifying magnetic coupling can be achieved by exchange coupling constant *J* calculations [20, 29, 32]. In the framework of density functional theory (DFT), the *J* constant is generally extracted from high spin (HS) and broken symmetry (BS) state energy computations [23–27, 48–55]. This technique introduced initially by Noodlemann et al. [56–58] was successfully used in combination with the hybrid B3LYP

functional, in the case of molecular radicals [15–19] and polynuclear d-transition and mixed 4*f*–*d* complexes [16, 20–46]. During last decade, much progress has been obtained in elucidation of magneto-structural correlations [32–36, 43, 46]. In the case of actinide compounds, it must be noted the renewed interest for some bi- and trimetallic species that could exhibit magnetic properties [59–62]. Indeed, recent studies have shown that they can also potentially be exploited in producing SMMs [60]. Furthermore, such systems are of fundamental interest owing to the involvement of the actinide 5*f* electrons in magnetic exchange interactions to be compared to the 4*f* orbitals of lanthanides [59, 60]. Although an important number of examples of these actinide-containing molecules featuring clear signature of magnetic exchange coupling have been reported [63–89], their theoretical study remains a challenge for quantum chemistry methods as stressed by Rinehart et al. [62].

A successful strategy in promoting interactions between actinide metallic ions has been the use of covalently linked bridging ligands. Indeed, magnetic coupling is attributed to indirect exchange interactions between spin centres connected by bridging functionalized ligands [60–63, 77, 78]. Thus, the use of an aromatic spacer bearing two functionalized metallic centres and combined with the radial extension of 5*f* orbitals should facilitate significant metal–metal electronic and magnetic interactions. For example, the imido linkage (imido = phenylenediimido ligand) was the first used in the diuranium(V) para-imido $[(MeC_5H_4)_3U]_2$ (μ-1,4-$N_2C_6H_4$) complex which exhibits a significant antiferromagnetic $5f^1$–$5f^1$ coupling [63]. Since a number of fascinating binuclear uranium(III), (IV) and (V) systems have been synthesized and their magnetic properties brought to light by experimental susceptibility measurements [64–89]. These systems include the binuclear amide complex $[U(\eta^8\text{-}C_8H_8)]_2[\mu\text{-}\eta^4\text{:}\eta^4\text{-}HN(CH_2)_3N(CH_2)_2N(CH_2)_3NH]$ [79], arene bridging diuranium(III) complexes, such as $[(Mes(^tBu)N)_2U]_2(\mu\text{-}\eta^6\text{:}\eta^6\text{-}C_7H_8)$ and $[(Cp^*)_2U]_2(\mu\text{-}\eta^6\text{:}\eta^6\text{-}C_6H_6)$ systems [85], cyclooctatetraene $(\mu\text{-}\eta^8\text{:}\eta^8\text{-}C_8H_8)U_2[NC(^tBu)MesN]_6$ (Mes = 2,4,6-$C_6H_2Me_3$) [84], polyuranyl UO_2^+ complexes [87], trimetallic actinide complex $[Cp^*_2An\{N{=}C(Bz)(tpy\text{-}An'Cp^*_2)\}_2]$ exhibiting mixed valency (An=Th^{IV}, An′=U^{IV}) [88] and Pyrazolate-bridged $[U(Me_2Pz)_4]_2$ (Me_2Pz = 3,5-dimethylpyrazolate) [71] diuranium(IV) complexes, are also likely to exhibit interesting magnetic properties.

Furthermore, recent reports in synthetic efforts toward paramagnetic actinide-containing assemblies indicate that ketimide (1,4-phenylenediketimide) ligands could lead to diverse and interesting magnetic behaviours [74–77]. Consequently, simple bis(ketimide) $[(C_5Me_4Et)_2(Cl)An]_2$ (μ-{N=CMe-(C_6H_4)-MeC=N}) binuclear An^{IV}/An^{IV} (Th, U) complexes [75] were synthesized; in the uranium case, metal–metal electronic communication could occur between the two $5f^2$–$5f^2$ spin centres through the aromatic spacer ligand.

More recently, a para- and meta-diethynylbenzene (DEB) bridging ligand have been used in binuclear isovalent U(IV)/U(IV) complexes with $[(NN'_3)_2U_2(DEB)]$ formula [78]. Experimental and theoretical DFT investigations of their magnetic properties have shown that both isomers exhibit a rather weak ferromagnetic and antiferromagnetic character for meta- and para-DEB, respectively [78]. A new bis(imido) diuranium(V) complex $[U(N^tBu)_2(I)(^tBu_2bpy)]_2$ exhibiting an moderate antiferromagnetic coupling between two metallic $5f^1$–$5f^1$ spin active centres has been synthesized and theoretically investigated [77]. For this system, B3LYP calculations predicted correctly that the BS state is lower in energy than the triplet HS state, providing an exchange coupling constant J (-12 cm^{-1}) in agreement with the experimental fitting of susceptibility measurements.

As aforementioned, exploiting and modelling the magnetic properties of actinide complexes still require a fundamental understanding of how to promote and modulate electronic delocalization and magnetic exchange interactions between spin centres [59–89]. In addition to this fundamental interest, the actinide coordination chemistry features a rich interplay of metal-bonding interactions, substitution pattern and the type of π network bridging ligand effects, whose understanding is crucial to the development of actinide magneto-structural chemistry and to settle longstanding questions about the role of 5*f* orbitals in metal–metal electronic and magnetic interactions through aromatic spacers [62].

In this work, we are particularly interested in the $[Cp'_2UCl]_2$(μ-ketimide) diuranium(IV) complexes (Cp' = C_5Me_4Et; ketimide = 1,4-phenylenediketimide) [75, 77] for which no systematic theoretical study has been carried out up to now, to our knowledge. This interesting system contains two active $5f^2$ electrons per centre connected by the bis(ketimide) aromatic π-spacer (Fig. 1). Experimentally, an antiferromagnetic character is expected for the complex in question, but was not completely brought to light by susceptibility measurements, while as judged by voltammetry, 'the complex displays appreciable electronic communication between the metal centres through the

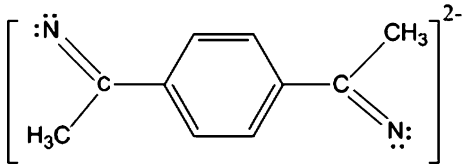

Fig. 1 The dianionic bis(ketimide) ligand

π-system of the dianionic diketimide bridging ligand' [75]. We have recently carried out [90] relativistic DFT investigations on bis(imido) diuranium ($5f^1$–$5f^1$) complexes in the framework of the zero order regular approximation (ZORA) predicting ferromagnetic and antiferromagnetic coupling, respectively, for the meta- and para-bis(imido) isomers, in agreement with experimental data [60, 63]. These results encouraged us to apply the same methodology to study the magnetic exchange interactions for the above mentioned diuranium(IV) ketimide system. Our theoretical study is likely to help the experimentalists in their investigations.

We shall first consider a model system henceforward called U_2ketimide where the Cp′ ligand of the complex has been replaced by an unsubstituted Cp ring and then the actual complex. The driving role of the aromatic spacer, that is, the bis(ketimide) bridging ligand and that of the uranium(IV) 5*f* orbitals, will be particularly investigated. As suggested by the authors of ref. 20b, we shall also consider its hypothetical congener ThUketimide complex that has not yet been isolated experimentally, in order to study the effect of replacing one paramagnetic U(IV) $5f^2$ centre by a diamagnetic Th(IV) $5f^0$ one.

2 Description of the model and computational details

The magnetic interaction between two atomic spins is usually described by the phenomenological Hamiltonian of Heisenberg, Dirac and Van Vleck (HDvV) [28–31, 91, 92] given by $\hat{H} = -2\,J\hat{S}_1 \cdot \hat{S}_2$, where $\hat{S}_1$ and $\hat{S}_2$ are the respective local spin angular momentum operators. A positive sign of the coupling constant *J* indicates a ferromagnetic interaction (parallel alignment of spins), whereas the negative sign indicates an antiferromagnetic interaction (anti parallel alignment of spins). It must be noted that to estimate the coupling constant *J*, one has to calculate energy differences that are often smaller than $\sim$0.5 kcal/mol (few tens cm^{-1}) [24, 29]. Accurate quantum mechanical evaluation of the coupling constant requires the use of multideterminantal post-Hartree–Fock calculations [24, 93]. However, such ab initio methodology is computationally challenging for great size systems and its use is reduced to small molecules or simplified models [93]. An alternative is provided by the DFT/BS approach [14] which has been proved to be one of the most efficient tools to investigate the magnetic properties of transition metal complexes [16, 20–46, 94–97]. In numerous cases, good agreement has been achieved with the experimental data using the BS recipe in conjunction with the B3LYP functional [98, 99]. In some cases, a mixing of Hartree–Fock exchange between 33% and 50% was found to lead to better results than the 20% used in B3LYP ([49] and ref. therein).

All computational results reported in this work were performed using the Amsterdam Density Functional (ADF2010.02 release) program [100]. Relativistic corrections have being introduced via the zero order regular approximation (ZORA) [101–104] accounting for scalar relativistic effects. Spin–orbit corrections to the energy difference between the high spin (HS) and BS states have not been considered. These corrections are of atomic nature [105–112], that is, not very sensitive to the environment of the metal ion for a given oxidation state. In the present study, the metal electron configuration is $5f^2$ for each U(IV) ion, whatever the HS or BS state, so that neglecting spin–orbit corrections seems to be a valid assumption. Recent DFT calculations of magnetic exchange coupling for biuranium(IV) and (V) species [77, 78, 90] did not also include spin–orbit corrections.

The GGA Becke–Perdew (BP86) [113, 114] and B3LYP hybrid functionals have been used. For all elements, Triple–ζ Slater-type valence orbitals (STO) augmented by one set of polarization functions were used taken from the ADF/ZORA/TZP database. The frozen-core approximation where the core density is obtained from four-component Dirac–Slater calculations has been applied for all atoms in the case of BP86 calculations: 1*s* core electrons were frozen, respectively, for carbon C[1*s*], nitrogen N[1*s*] and Cl[2*p*]. The actinide U[5*d*] valence space of the heavy elements includes the 5*f*/6*s*/6*p*/6*d*/7*s*/7*p* shells (14 valence electrons). The B3LYP computations are all electron ones.

Our previous work [105–109] and several recent studies [68, 69, 116–120] have shown that ZORA/BP86/TZP computations reproduce experimental geometries and ground state properties of f–element compounds with a satisfying accuracy.

It is noteworthy that several stages were needed to obtain converged results observing an aufbau electron configuration with the electronic structure $5f^2$–$5f^2$ for the U_2ketimide binuclear complex under consideration. The HS state geometry optimization at the ZORA/BP86/TZP level has been carried out first; the smearing procedure implemented in ADF, permitting a fractional occupation of the 5*f* orbitals by the four unpaired electrons ($5f^2$–$5f^2$), was turned on. Then, the electron smearing was progressively reduced until reaching the required 5*f* electrons distribution. Finally, the BS state energy (E_{BS}) has been obtained performing a single point calculation using the MOs of the HS structure as starting guess and changing the spin on the second uranium atom.

Molecular structure drawings, spin densities and molecular orbital plots were generated using the ADF-GUI auxiliary program [100].

3 Results and discussion

3.1 Description of the molecular geometries

The ketimide (1,4-phenylenediketimide) dianionic ligand (Fig. 1) has shown through recent spectroscopic and electronic structure reports [74–77, 115, 119, 120], a great ability to promote ligand–metal charge transfer. It proved also to be an efficient bridging ligand for high-nuclearity molecular frameworks [88]. In our case, the greater radial extension of the 5*f* valence orbitals of uranium can potentially provide increased overlap with the bridging ligand, as a result of the U(5*f*)–N π-bonding interaction that involves the nitrogen lone pair, thereby enhancing the communication between the bridged metal centres [77, 90].

As aforementioned, our targeted systems are the bimetallic model $[(Cp)_2UCl]_2(\mu$-ketimide) called U_2ketimide complex, $[(C_5Me_4Et)_2UCl]_2(\mu$-ketimide) the X-ray characterized [75] one and the hypothetical ThUketimide species. In order to compare the homobimetallic U(IV)/U(IV) U_2ketimide and the mixed Th(IV)/U(IV) ThUketimide complexes, their molecular geometries were fully optimized in C_s symmetry at the ZORA/BP86/TZP level. The optimized geometries have been obtained considering the HS triplet $5f^0$–$5f^2$ ($S = 1$) and quintet $5f^2$–$5f^2$ ($S = 2$) spin states for the ThUketimide and U_2ketimide, respectively. The obtained molecular structures of the model ThUketimide and U_2ketimide complexes are depicted on Fig. 2.

In Table 1 are given relevant optimized bond distances and angles of the ThUketimide and U_2ketimide model complexes, respectively, in their triplet and quintet HS state in the C_s symmetry. Available X-ray structural parameters for the experimental $[(C_5Me_4Et)_2UCl]_2(\mu$-ketimide) and $[(C_5Me_5)_2ThCl]_2(\mu$-ketimide) complexes [75] are also given in this table. The given geometrical parameters are defined on Fig. 2.

As it can be seen in Table 1, there is a good overall agreement between the optimized geometry of the U/U species and the available X-ray structure, reminding that the latter bears more crowded C_5Me_4Et ligands [75] explaining partly why the U–N computed distance is underestimated. Furthermore, comparing the two Th/U and U/U optimized structures, it can be seen that differences in metal–ligand bond lengths are partly due to Th(IV) vs. U(IV) ionic radii variations, the radius of Th(IV) being 0.05 Å larger than the U(IV) one [121] but also to the bonds covalent character which is higher for uranium.

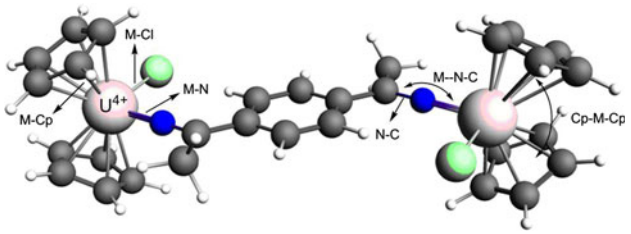

Fig. 2 Relevant structural parameters (values in Table 1)

From Table 1, it is noteworthy that U–N bond distances are in the range of multiple short bonds in agreement with experimental structural data of analogues ketimide or imido complexes found in the literature [74–77, 106, 115, 122]. The quasi-linear U–N–C coordination is also indicative of multiple bonding. Such coordination in the diuranium(IV) complex, throughout the ketimide (1,4-phenylenediketimide) bridging ligand, which appears also in bis(imido) diuranium(V) species [63, 90], is likely to maximize the possibility of electronic and magnetic communication between the two metallic centres. Different authors [106, 115, 120] attributed this peculiar linear U–N–C coordination, to a significant participation of the uranium 5*f* orbitals in metal–N bonding. This U–N(ketimide) coordination exhibits both σ and π interactions between the central metal and bis(ketimide) bridging ligand via the nitrogen electron pairs. We expect also that the 5*f* uranium orbitals are not only responsible for this peculiar geometry, but could play a key role in magnetic exchange interaction cooperatively with the π-conjugated aromatic spacer. This point will be supported by the MO analysis which follows.

3.2 DFT evaluation of the exchange coupling constant *J*

We study now the magnetic character of the complexes under consideration starting from the U_2ketimide model and $[Cp'_2UCl]_2(\mu$-ketimide) the X-ray characterized complex. We remind that the antiferromagnetic character of the latter was not clearly evidenced experimentally by variable temperature measurements [75]. The study of the hypothetical ThUketimide complex will come after. The U_2ketimide systems exhibiting the $5f^2$–$5f^2$ configuration will be considered in its HS(↑↑–↑↑) and BS(↑↑–↓↓) states.

On the basis of the HDvV Hamiltonian ($\hat{H} = -2\,J\hat{S}_1 \cdot \hat{S}_2$), exchange coupling constant J can be extracted from the energy difference $\Delta E = E_{BS} - E_{HS}$ of the HS and BS states [32–58]. According to the spin-projected (SP) approach [56], the energies of a two-centre A and B complex can be related to the J coupling as:

$$J_{AB} = (E_{BS} - E_{HS})/2S_AS_B \quad (1)$$

while in the non-spin-projected (NP) approach [32], the corresponding energies can be related to the J coupling as:

$$J_{AB} = (E_{BS} - E_{HS})/(2S_AS_B + S_B) \quad (2)$$

where S_A and S_B are the total local spin angular momenta. In our case, $S_A = S_B = 1$ so that Eqs. 1 and 2 lead,

Table 1 Relevant average optimized computed bond (Å) distances and angles (°) of U_2ketimide (U/U) and ThUketimide (Th/U) complexes at the ZORA/BP86/TZP level and X-ray values

M/M′	M–N	M–Cl	N–C	M–M	M–Cp	M–N–C	Cp–M–Cp
U/U	2.088	2.609	1.307	11.057	2.472	178.6	125.1
X-ray	2.250(2)	2.710(13)	1.260(3)	10.956	2.471–2.493	175.3	140.2
Th/U	2.219/2.104	2.666/2.580	1.275/1.296	11.034	2.564/2.458	179.8/179.2	126.8/125.5

Available X-ray structural parameters are for $[(C_5Me_4Et)_2UCl]_2(\mu$-ketimide)

respectively, to $J = \Delta E/2$ and $J = \Delta E/3$. Several authors argued that Eq. 1 represents the more physically meaningful mapping between the HDvV and the DFT/BS models [48, 92].

In addition, the Yamaguchi et al. spin-projected method [94] lead to the following expression of J (3):

$$J_{AB} = (E_{BS} - E_{HS})/\langle S^2\rangle_{HS} - \langle S^2\rangle_{BS} \quad (3)$$

where $\langle S^2\rangle_{HS}$ and $\langle S^2\rangle_{BS}$ are the mean values of the $\hat{S}^2$ squared spin operator, respectively, for the HS and BS states.

To investigate the effect of a small geometry modification on the computed properties, we computed, in addition to the U2ketimide model in its optimized structure, the actual $[Cp'_2UCl]_2(\mu$-ketimide) diuranium(IV) complex using its X-ray geometry [75]. In Table 2 are reported the computed $\Delta E = E_{BS} - E_{HS}$ energy differences, the mean values $\langle S^2\rangle$ of the squared spin operator and the computed exchange coupling constants $J(cm^{-1})$ using the three above-mentioned different expressions. In this table, computed values for the actual complex and the U2ketimide model have been obtained by means of the BP86 functional and the B3LYP one.

$\langle S^2\rangle$ exhibits the expected values, that is, of the order of 2 for the BS and 6 for the HS states; moreover, a weak spin contamination for the HS state can be noticed. An important observation from the results of Table 2 is that, contrarily to B3LYP, the BP86 functional leads to very high energy differences between the HS and BS states. As stressed by previous authors [32–36, 41–46, 48–55], the resulting values of the exchange coupling constant J, in the GGA case, are systematically larger in absolute values, than those expected for such systems [62, 63, 77, 78]. We noticed the same overestimation using another GGA functional.

We note that B3LYP predicts a rather weak antiferromagnetic character either for the actual complex (-1.7 to -3.4 cm^{-1}) or the U2ketimide model (from -2.3 to -4.6 cm^{-1}). To our knowledge, no coupling constant values have been published up to now for these complexes, so that a direct comparison is not possible. However, such small values of J are not unexpected for bimetallic uranium(IV) complexes [78]. Moreover, it is worth noting that the coupling constants in the case of a U(V)–U(V) $5f^1$–$5f^1$ binuclear complex like para-bis(imido) $[(C_5H_5)_3U]_2$ (μ-imido) uranium(V) are higher in absolute value than for the considered U(IV) $5f^2$–$5f^2$ complexes [60, 90].

The magnetic character of binuclear complexes can be well explained considering the spin density distributions in the HS and BS states, as already demonstrated by several authors [20, 23, 37–40, 72, 78]. Some mechanisms have been proposed to explain the exchange coupling between magnetic centres, that is, the spin polarization and spin delocalization effects, phenomena well known in the case of d-transition metals magneto-chemistry [37–40, 49, 93–97] described early by O. Kahn [47].

The obtained spin density distributions (differences between α and β electron densities) for the U_2ketimide model complex are displayed on Fig. 3.

We note that the HS state exhibits quasi-localized spin densities on the two magnetic uranium centres with non-negligible values on their nearest neighbours but no spin delocalization within the phenyl ring. On the contrary, the BS spin density distribution shows that the two magnetic

Table 2 ΔE (eV and cm^{-1}) energy differences, $\langle S^2\rangle$ values and computed exchange coupling J(cm^{-1}) constant for the U_2ketimide model (optimized geometry) and actual complex (X-ray structure)

Diuranium complex	$\Delta E_{(BS-HS)}$ cm^{-1}	$\langle S^2\rangle_{HS}$	$\langle S^2\rangle_{BS}$	$J^{(1)}$	$J^{(2)}$	$J^{(3)}$
U_2ketimide model						
BP86	−437.2	6.073	1.942	−218.1	−145.1	−105.8
B3LYP	−9.3	6.038	2.039	−4.6	−3.1	−2.3
Actual complex						
BP86	−680.4	6.095	2.044	−340.2	−226.8	−170.1
B3LYP	−6.9	6.046	2.047	−3.4	−2.3	−1.7

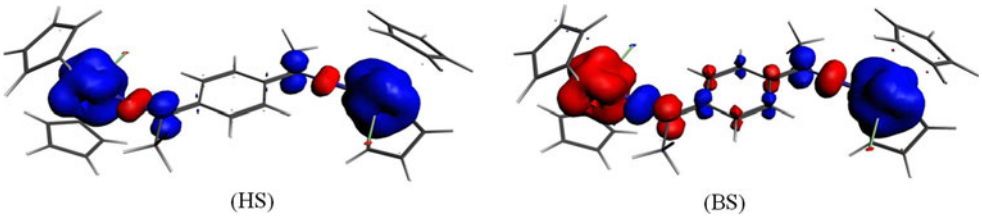

Fig. 3 ZORA/B3LYP spin density distributions for the HS (quintet) and BS states of U_2ketimide complex (blue colour: positive and red colour: negative spin density). The isodensity surface corresponds to a value of 0.0025 e bohr^{-3}

centres are antiferromagnetically coupled, with significant spin density contributions from all bis(ketimide) ligand atoms. The sign alternation of the spin densities along the path linking the two magnetic centres, due to spin polarization, proves the exchange coupling. It is worth noting that, due to the even number of atoms constituting the latter path, only an antiferromagnetic interaction due to spin polarization is possible. We observed the same behaviour in the case of $5f^1$–$5f^1$ bis (imido) uranium complexes [90]; the para isomer for which the bridging path between the magnetic centres contains an even number of atoms is antiferromagnetic, whereas the meta one, containing an odd number of linking atoms, is ferromagnetic. In the latter case, the sign alternation of the spin densities along the bridge is obtained for the HS state of the complex. So, the topology of the linking path determines the magnetic character driven by spin polarization, of such binuclear complexes.

We note that the Cp ligands are practically not involved in this coupling, clarifying partly why the U2ketimide model, that is, $[Cp_2UCl]_2(\mu$-ketimide) and the actual complex bearing substituted Cps, $[(C_5Me_4Et)_2UCl]_2$ (μ-ketimide) lead to very close J values. The antiferromagnetic coupling is also clarified by the alternating signs of the atomic Mulliken spin polarizations (difference of the α and β gross atomic charges) found in the BS state along the path linking the two magnetic metal centres as given in Table 3. Despite its known drawbacks, the Mulliken population analysis remains a useful tool to compare the variation of electronic populations in homologous series of compounds computed at the same level of theory.

In Table 3, atoms are numbered as indicated on Fig. 4; the computed values for the X-ray structure are given between parentheses.

As expected on the basis of the electron spin density distributions, the atomic spin polarizations of the atoms of the linking bridge increase significantly in absolute values when passing from the HS to BS state. This confirms the crucial rule of the bridging ligand to promote metal–metal electronic communications leading to exchange coupling interactions within an antiferromagnetic state. It is also interesting to note that that the model complex and the actual one exhibit almost the same spin populations in the HS state, whereas they differ slightly in the BS state.

Table 3 ZORA/B3LYP Mulliken spin populations for HS and BS states of U_2ketimide model complex (computed values for the actual complex given between parentheses)

U_2ketimide	HS		BS	
Atoms				
U1	2.148	(2.174)	2.146	(2.172)
Cl2	−0.043	(−0.042)	−0.041	(−0.022)
N3	−0.090	(−0.087)	−0.129	(−0.110)
C4	0.136	(0.131)	0.126	(0.114)
C5	−0.017	(−0.016)	−0.047	(−0.036)
C6	−0.013	(−0.010)	−0.057	(−0.039)
C7	0.018	(0.016)	0.037	(0.021)
C8	0.013	(0.011)	−0.043	(−0.022)
C9	−0.013	(−0.014)	0.057	(0.029)
C10	0.011	(0.012)	−0.037	(−0.021)
C11	0.013	(0.010)	0.043	(0.022)
C12	0.136	(0.110)	−0.126	(−0.114)
C13	−0.017	(−0.012)	0.017	(0.015)
N14	−0.090	(−0.087)	0.129	(0.110)
U15	2.149	(2.174)	−2.147	(−2.172)
Cl16	−0.044	(−0.042)	0.041	(0.022)

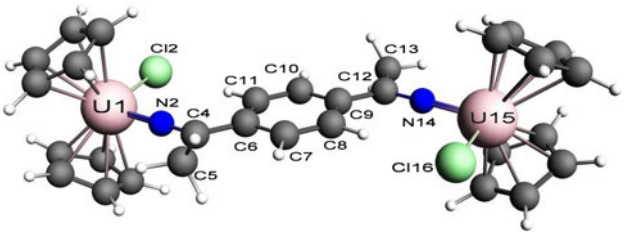

Fig. 4 Atom numbering of the U_2ketimide model

The effect of the replacement of one paramagnetic metal U($5f^2$) by a diamagnetic Th($5f^0$) one on the atomic spin populations appears in Table 4 (same atoms numbering as Fig. 3) where are reported these values for the Th^{IV}/U^{IV} ThUketimide hypothetical complex. We remind that such mixed metal complex, which has not yet been isolated experimentally, is designed to estimate the coupling constant in the U/U complex [75] by diamagnetic subtraction analysis [60].

Table 4 ZORA/B3LYP Mulliken spin populations of the ThUketimide model complex

Atoms	U1	Cl2	N3	C4	C5	C6	C7	C8	C9	C10	C11	C12	C13	N14	Th15	Cl16
	2.125	−0.023	−0.046	0.004	−0.002	−0.003	0.000	0.000	0.000	0.000	0.000	0.000	0.000	0.000	0.000	0.000

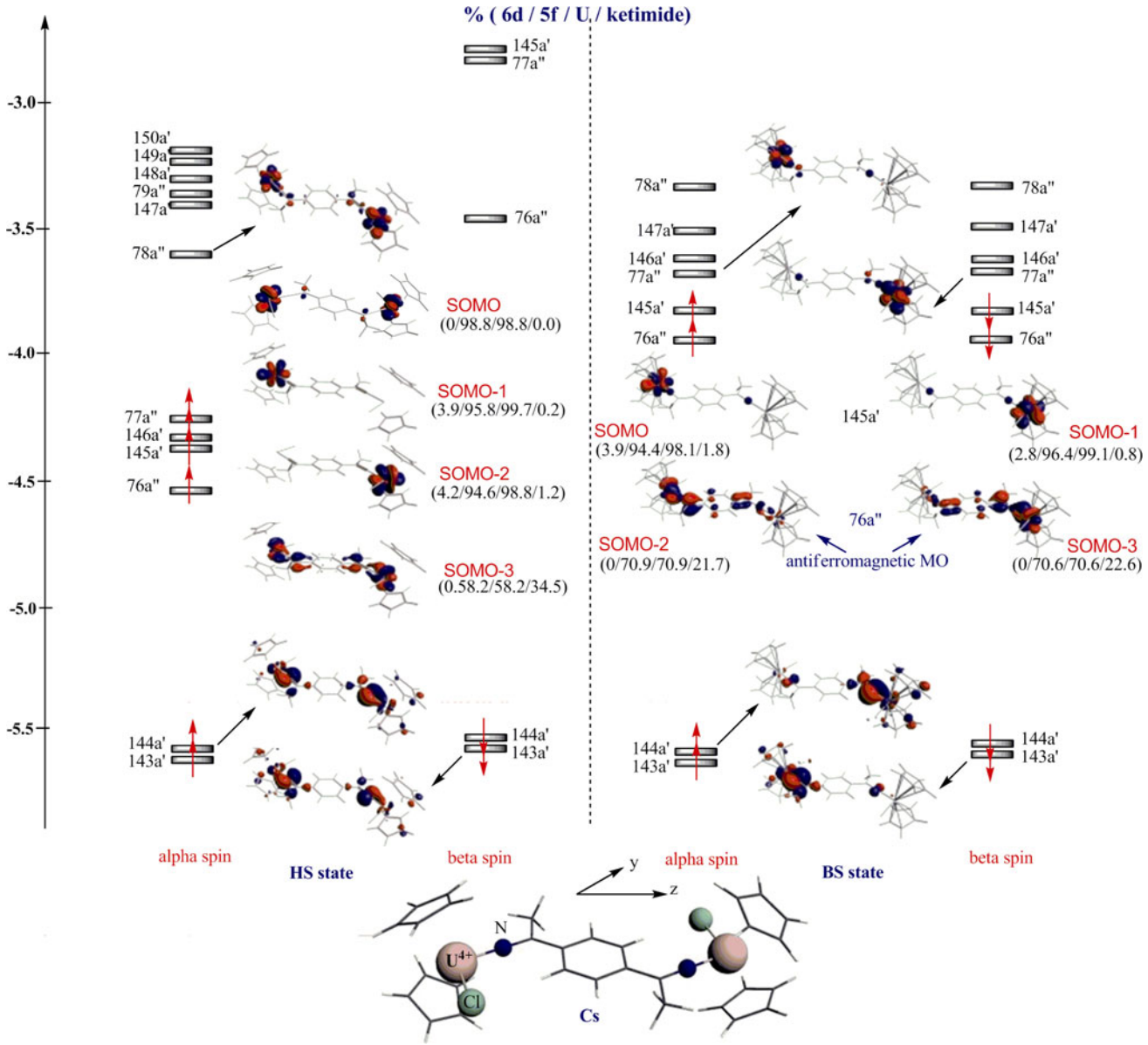

Fig. 5 B3LYP Frontier MO diagrams of HS and BS states for the U_2ketimide model complex in the $C_s(yz)$ symmetry

From results of Table 4, it can be seen that the spin populations are equal to zero for thorium, the chlorine and nitrogen atoms directly bonded to it and for the atoms of the bridging ligand. Cl2 and N3 atoms, linked to the paramagnetic U(IV) ion, are the only ones for which the spin populations are relatively high with negative values owing to the spin polarization effect from the U(IV) spin centre. This mixed system illustrates well that replacing the paramagnetic centre U(IV) by its diamagnetic analogue Th(IV) affects drastically the spin polarization effect; the spin densities tend to zero beyond the first neighbours of the paramagnetic centre. Obviously, no magnetic exchange interaction could occur in such system.

The MO diagram of the U2ketimide model in $C_s(yz)$ symmetry depicted on Fig. 5 displays the singly occupied molecular orbitals (SOMOs) of the HS state at the left side, with the corresponding BS SOMOs at the right side. In this diagram, %(6*d*/5*f*/U/ligand) represents the weight of,

respectively, the 6*d*, 5*f* orbitals, the uranium atoms and the bridging ligand within the displayed MOs.

In the HS quintet state, the four highest α SOMOs, SOMO-3 (76a″) excepted, that is, SOMOs #77a″, 145a′ and 146a′, are essentially 5*f* orbitals of the two uranium(IV) atoms with no contribution from the bridging ketimide ligand. On the contrary, in the BS state, SOMOs # α-76a″ and *β*-76a″ are significantly different and appear to be more delocalized with non-negligible contribution of the bis(ketimide) ligand as testified by the orbital percentages. In the BS state, two different pairs of molecular levels can be distinguished; the first one of a′ symmetry is essentially of localized 5*f* character, the second, with a″ symmetry and, combining α and *β* spin-parts, is rather well delocalized over the path linking the two spin centres U(IV). This picture agrees well with the spin density distribution, depicted on Fig. 4. Immediately below, MOs #144 and 143, with a′ symmetry, remain unchanged when passing from HS to BS state. These MOs of bonding character exhibit large *π*-bonding interactions, involving uranium 5*f* orbitals and *π*-orbitals of the N-bridging atoms. The experimentally observed electronic communication between the two uranium atoms is also well described by the MO description of the complex.

4 Conclusions

The magnetic exchange coupling interactions in bis(ketimide) $[(C_5H_5)_2(Cl)An]_2(\mu$-{N=CMe-(C_6H_4)-MeC=N}) and $[(C_5Me_4Et)_2UCl]_2(\mu$-ketimide) binuclear U^{IV}/U^{IV} complexes exhibiting the $5f^2$–$5f^2$ electron configuration have been investigated theoretically for a first time using relativistic DFT/ZORA computations combined with the broken symmetry approach. ZORA/B3LYP computations predict a rather weak antiferromagnetic coupling constant $|J| < 5\ cm^{-1}$. Not surprisingly, the BP86 GGA functional overestimating the $|J|$ values fails to predict the weak antiferromagnetic character of the U_2ketimide complex. The magnetic exchange coupling has been rationalized considering spin density distributions and Mulliken atomic spin populations. The antiferromagnetic coupling is clarified by the alternating signs of the atomic spin populations along the path linking the two magnetic metal centres occurring in the BS state. The fact that the number of atoms along the path linking the two metal ions is even leads to antiferromagnetic coupling, the latter being mainly due to spin polarization. Furthermore, from the MO point of view, the antiferromagnetic interaction between the two uranium(IV) ions mediated by the aromatic ketimide bridge is mainly due to the effective *π*-overlap between 5*f* orbitals and nitrogen atoms on bridging ligand groups along the path linking the two magnetic uranium(IV) centres.

Acknowledgments Financial support from the Algerian National Administration of Scientific Research NASR-ANDRU (PNR Grant No. 8/u250/4169) is gratefully acknowledged. Computing facilities were provided by IDRIS Computing Centre of CNRS.

References

1. Bencini A, Benelli C, Caneschi A, Carlin RL, Dei A, Gatteschi D (1985) J Am Chem Soc 107:8128–8136
2. Benelli C, Gatteschi D (2002) Chem Rev 102:2369–2387
3. Sessoli R, Gatteschi D (2003) Angew Chem Int Ed 42:268–297
4. Long JR (2003) Molecular cluster magnets. In: Yang P (ed) Chemistry of nanostructured materials. World Scientific, Hong Kong, pp 291–315
5. Sessoli R, Tsai HL, Schake AR, Wang SY, Vincent JB, Folting K, Gatteschi D, Christou G, Hendrickson DN (1993) J Am Chem Soc 115:1804–1816
6. Sessoli R, Gatteschi D, Caneschi A, Novak MA (1993) Nature 365:14–143
7. Osanai K, Okazawa A, Nogami T, Ishida T (2006) J Am Chem Soc 128:14008–14009
8. Atakol O, Boca R, Ercan I, Ercan F, Fuess H, Haase W, Herchel R (2006) Chem Phys Lett 423:192–196
9. Calzado CJ, Clemente-Juan JM, Coronado E, Gaita-Arino A, Suaud N (2008) Inorg Chem 47:5889–5901
10. Kim JI, Kwak HY, Yoon JH, Ryu DW, Yoo IY, Yang N (2009) Ki Cho B, Park JG, Lee H, Hong CS. Inorg Chem 48:2956–2966
11. Andruh M, Costes JP, Diaz C, Gao S (2009) Inorg Chem 48:3342–3359
12. Affronte M, Troiani F, Ghirri A, Carretta S, Santini P, Corradini V, Schuecker R, Muryn C, Timco G, Winpenny RE (2006) Dalton Trans:2810–2817
13. Milios CJ, Inglis R, Vinslava A, Bagai R, Wernsdorfer W, Parsons S, Perlepes SP, Christou G, Brechin EK (2007) J Am Chem Soc 129:12505–12511
14. Bogani L, Wernsdorfer W (2008) Nat Mater 7:179–186
15. Adamo C, Barone V, Subra R (2000) Theor Chem Acc 104:207–209
16. Barone V, Bencini A, Gatteschi D, Totti F (2002) Chem Eur J 8:5019–5027
17. Barone V, Cacelli I, Ferretti A (2009) J Chem Phys 130:094306–094309
18. Barone V, Bloino J, Biczysko M (2010) Phys Chem Chem Phys 12:1092–1101
19. Pavone M, Biczysko M, Rega N, Barone V (2010) J Phys Chem B 114:11509–11514
20. Ferrando-Soria J, Castellano M, Yuste C, Lloret F, Julve M, Fabelo O, Ruiz-Pérez C, Stiriba SE, Ruiz-García R, Cano J (2010) Inorg Chim Acta 363:1666–1678
21. Labéguerie P, Rohmer MM, Bénard M (2009) J Chin Chem Soc 56:22–25
22. Ismayilov RH, Wang WZ, Lee GH, Yeh CY, Hua SA, Song Y, Rohmer MM, Bénard M, Peng SM (2011) Angew Chem Int Ed 50:2045–2048
23. Gillon B, Mathonire C, Ruiz E, Alvarez S, Cousson A, Rajendiran TM, Kahn O (2002) J Am Chem Soc 124:14433–14441
24. Ciofini I, Daul CA (2003) Coord Chem Rev 238–239:187–209
25. Costuas K, Valenzuela ML, Vega A, Moreno Y, Pena O, Spodine E, Saillard JY, Diaz C (2002) Inorg Chim Acta 329:129–134
26. Kortus J (2007) C R Chimie 10:65–67
27. Castro I, Calatayud ML, Sletten J, Lloret F, Julve M (1997) Dalton Trans:811–818
28. Fink K, Fink R, Staemmler V (1994) Inorg Chem 33:6219–6229

29. Bencini A, Costes JP, Dahan F, Dupuis A, Garcia-Tojal J, Gatteschi D, Totti F (2004) Inorg Chim Acta 357:2150–2156
30. Albonico C, Bencini A (1988) Inorg Chem 27:1934–1940
31. Korzeniak T, Desplanches C, Podgajny R, Giménez-Saiz C, Stadnicka K, Rams M, Sieklucka B (2009) Inorg Chem 48:2865–2872
32. Ruiz E, Cano J, Alvarez S, Alemany P (1999) J Comput Chem 20:1391–1400
33. Ruiz E, Rodríguez-Fortea A, Cano J, Alvarez S, Alemany P (2003) J Comput Chem 24:982–989
34. Ruiz E, Rodriguez-Fortea A, Tercero J, Cauchy T, Massobrio CJ (2005) Chem Phys 123:074102–074110
35. Nunzi F, Ruiz E, Cano J, Alvarez S (2007) J Phys Chem C 111:618–621
36. Ruiz E, Cauchy T, Cano J, Costa R, Tercero J, Alvarez S (2008) J Am Chem Soc 130:7420–7426
37. Noh EAA, Zhang J (2006) Chem Phys 330:82–89
38. Noh EAA, Zhang J (2008) J Mol Struct THEOCHEM 867:33–38
39. Noh EAA, Zhang J (2009) J Mol Struct THEOCHEM 896:54–62
40. Yan F, Chen Z (2000) J Phys Chem A 104:6295–6300
41. Adamo C, Barone V, Bencini A, Totti F, Ciofini I (1999) Inorg Chem 38:1996–2004
42. Adamo C, Barone V, Bencini A, Broer R, Filatov M, Harrison NM, Illas F, Malrieu JP (2006) Moreira IdPR. J Chem Phys 124:107101–107103
43. Atanasov M, Comba P, Daul CA (2006) J Phys Chem A 110:13332–13340
44. Atanasov M, Comba P, Daul CA (2008) Inorg Chem 47:2449–2463
45. Atanasov M, Comba P, Hausberg S, Martin B (2009) Coord Chem Rev 253:2306–2314
46. Comba P, Hausberg S, Martin B (2009) J Phys Chem A 113:6751–6755
47. Kahn O (1993) Molecular Magnetism. VCH, New York
48. Moreira IdPR, Costa R, Filatov M, Illas F (2007) J Chem Theory Comput 3:764–774
49. Bencini A (2008) Inorg Chim Acta 361:3820–3831
50. Neese F (2009) Coord Chem Rev 253:526–563
51. Cramer CJ (2009) Truhlar D G. Phys Chem Chem Phys 11:10757–10816
52. Onofrio N, Mouesca JM (2011) Inorg Chem 50:5577–5586
53. Zhekova H, Seth M, Ziegler T (2011) J Chem Theory Comput 7:1858–1866
54. Peralta JE, Melo JI (2010) J Chem Theory Comput 6:1894–1899
55. Roy LE, Hughbanks T (2006) J Am Chem Soc 128:568–575
56. Noodleman LJ (1981) J Chem Phys 74:5737–5743
57. Noodleman LJ, Davidson ER (1986) Chem Phys 109:131–143
58. Noodleman LJ, Peng CY, Case DA, Mouesca JM (1995) Coord Chem Rev 144:199–244
59. Ephritikhine M (2006) Dalton Trans:2501–2516
60. Lukens WW, Walter MD (2010) Inorg Chem 49:4458–4465
61. Minasian SG, Krinsky JL, Rinehart JD, Copping R, Tyliszczak T, Janousch M, Shuh DK, Arnold J (2009) J Am Chem Soc 131:13767–13783
62. Rinehart JD, Harris TD, Kozimor SA, Bartlett BM, Long JR (2009) Inorg Chem 48:3382–3395
63. Rosen RK, Andersen RA, Edelstein NM (1990) J Am Chem Soc 112:4588–4590
64. Diaconescu PL, Arnold PL, Baker TA, Mindiola DJ (2000) Cummins C C. J Am Chem Soc 122:6108–6109
65. Fox AR, Bart SC, Meyer K, Cummins CC (2008) Nature 455:341–349
66. Jilek RE, Spencer LP, Kuiper DL, Scott BL, Williams UJ, Kikkawa JM, Schelter EJ, Boncella JM (2011) Inorg Chem 50:4235–4237
67. Roussel P, Errington W, Kaltsoyannis N, Scott P (2001) J Organomet Chem 635:69–74
68. Cloke FGN, Green JC, Kaltsoyannis N (2004) Organometallics 23:832–835
69. Gaunt AJ, Reilly SD, Enriquez AE, Scott BL, Ibers JA, Sekar P, Ingram KIM, Kaltsoyannis N, Neu MP (2008) Inorg Chem 47:29–41
70. Evans WJ, Montalvo E, Kozimor SA, Miller KA (2008) J Am Chem Soc 130:12258–12259
71. Kozimor SA, Bartlett BM, Rinehart JD, Long JR (2007) J Am Chem Soc 129:10672–10674
72. Monreal MJ, Carver CT, Diaconescu PL (2007) Inorg Chem 46:7226–7228
73. Rajaraman G, Totti F, Bencini A, Caneschi A, Sessoli R, Gatteschi D (2009) Dalton Trans 3153–3161
74. Schelter EJ, Veauthier JM, Thompson JD, Scott BL, John KD, Morris DE, Kiplinger JL (2006) J Am Chem Soc 128:2198–2199
75. Schelter EJ, Veauthier JM, Graves CR, John KD, Scott BL, Thompson JD, Pool-Davis-Tournear JA, Morris DE, Kiplinger JL (2008) Chem Eur J 14:7782–7790
76. Veauthier JM, Schelter EJ, Carlson CN, Scott BL, Da Re RE, Thompson JD, Kiplinger JL, Morris DE, John KD (2008) Inorg Chem 47:5841–5849
77. Spencer LP, Schelter EJ, Yang P, Gdula RL, Scott BL, Thompson JD, Kiplinger JL, Batista ER, Boncella JM (2009) Angew Chem Int Ed 48:3795–3798
78. Newell BS, Rapp AK, Shores MP (2010) Inorg Chem 49:1595–1606
79. Berthet JC, Ephritikhine M (1998) Coord Chem Rev 83:178–180
80. Borgne TL, Lance M, Nierlich M, Ephritikhine M (2000) J Organomet Chem 598:313–317
81. Le Borgne T, Rivière E, Marrot J, Thuéry P, Girerd JJ, Ephritikhine M (2002) Chem Eur J 8:773–783
82. Salmon L, Thuéry P, Rivière E, Girerd JJ, Ephritikhine M (2003) Dalton Trans:2872–2880
83. Salmon L, Thuéry P, Rivière E, Ephritikhine M (2006) Inorg Chem 45:83–93
84. Diaconescu PL, Cummins CC (2002) J Am Chem Soc 124:7660–7661
85. Evans WJ, Kozimor SA, Ziller JW, Kaltsoyannis N (2004) J Am Chem Soc 126:14533–14547
86. Monreal MJ, Diaconescu PL (2008) Organometallics 27:1702–1706
87. Nocton G, Horeglad P, Pécaut J, Mazzanti M (2008) J Am Chem Soc 130:16633–16645
88. Schelter EJ, Wu R, Scott BL, Thompson JD, Morris DE, Kiplinger JL (2008) Angew Chem Int Ed 47:2993–2996
89. Mills DP, Moro F, McMaster J, van Slageren J, Lewis W, Blake AJ, Liddle ST (2011) Nature Chemistry 3:454–460
90. Meskaldji S, Belkhiri A, Belkhiri L, Boucekkine A, Ephritikhine M (2011) C R Chimie (in press)
91. Caballol R, Castell O, Illas F, Moreira IP, Malrieu JP (1997) J Phys Chem A 101:7860–7866
92. Figgis BN, Hitchman MA (2000) Ligand field theory and its applications. Wiley, London
93. Fouqueau A, Casida ME, Daku LML, Hauser A, Neese F (2005) J Chem Phys 122:044110–044123
94. Mitani M, Mori H, Takano Y, Yamaki D, Yoshioka Y, Yamaguchi K (2000) J Chem Phys 113:4035–4051
95. Takano Y, Kitagawa Y, Onishi T, Yoshioka Y, Yamaguchi K, Koga N, Iwamura H (2002) J Am Chem Soc 124:450–461
96. Onishi T, Yamaki D, Yamaguchi K, Takano Y (2003) J Chem Phys 118:9747–9761

97. Shoji M, Koizumi K, Kitagawa Y, Kawakami T, Yamanaka S, Okumura M, Yamaguchi K (2006) Chem Phys Lett 432:343–347
98. Becke AD (1993) J Chem Phys 98:5648–5652
99. Lee C, Yang W, Parr RG (1988) Phys Rev B 37:785–789
100. ADF2010.02, SCM; Theoretical chemistry, Vrije University: Amsterdam, The Netherlands. http://www.scm.com
101. van Lenthe E, Baerends EJ, Snijders JG (1993) J Chem Phys 99:4597–4610
102. van Lenthe E, Baerends EJ, Snijders JG (1994) J Chem Phys 101:9783–9792
103. van Lenthe E, Ehlers A, Baerends EJ (1999) J Chem Phys 110:8943–8953
104. van Lenthe E, Snijders JG, Baerends EJ (1996) J Chem Phys 105:6505–6516
105. Elkechai A, Belkhiri L, Amarouche M, Clappe C, Boucekkine A, Hauchard D, Ephritikhine M (2009) Dalton Trans:2843–2849
106. Belkhiri L, Lissillour R, Boucekkine A (2005) J Mol Struct THEOCHEM 757:155–164
107. El Kechai A, Meskaldji S, Boucekkine A, Belkhiri L, Bouchet D, Amarouche M, Clappe C, Hauchard D, Ephritikhine M (2010) J Mol Struct THEOCHEM 954:115–123
108. Meskaldji S, Belkhiri L, Arliguie T, Fourmigué M, Ephritikhine M, Boucekkine A (2010) Inorg Chem 49:3192–3200
109. El Kechai A, Boucekkine A, Belkhiri L, Hauchard D, Clappe C, Ephritikhine M (2010) C R Chimie 13:860–869
110. Schreckenbach G, Shamov GA (2010) Acc Chem Res 43:19–29
111. Xiao H, Li J (2008) Chin J Struct Chem 27:967–974
112. García-Hernandez M, Lauterbach C, Krüger S, Matveev A, Rösch N (2002) J Comput Chem 23:834–846
113. Becke AD (1988) Phys Rev A 38:3098–3100
114. Perdew JP (1986) Phys Rev B 34:7406–7409
115. Graves CR, Yang P, Kozimor SA, Vaughn AE, Clark DL, Conradson SD, Schelter EJ, Scott BL, Thompson JD, Hay PJ, Morris DE, Kiplinger JL (2008) J Am Chem Soc 130:5272–5285
116. Fox AR, Creutz SE, Cummins CC (2010) Dalton Trans 39:6632–6634
117. Cavigliasso G, Kaltsoyannis N (2006) Inorg Chem 45:6828–6839
118. Shamov GA, Schreckenbach G (2005) J Phys Chem A 109:10961–10974
119. Schelter E J, Yang P, Scott BL, Thompson JD, Martin RL, Hay PJ, Morris DE, Kiplinger JL (2007) Inorg Chem 46:7477–7488
120. Clark AE, Martin RL, Hay PJ, Green JC, Jantunen KC, Kiplinger JL (2005) J Phys Chem A 109:5481–5491
121. Shannon RD (1976) Acta Crystallogr A 32:751–767
122. Brennan JG, Andersen R (1985) J Am Chem Soc 107:514–516